Supplementary Information for:

Understanding the Bias Dependence of Low Frequency Noise in Single Layer Graphene FETs

Nikolaos Mavredakis*[a], Ramon Garcia Cortadella[b], Andrea Bonaccini Calia[b], Jose A. Garrido[b] and David Jiménez[a]

[a] Departament d'Enginyeria Electrònica, Escola d'Enginyeria, Universitat Autònoma de Barcelona, Bellaterra 08193, Spain

[b] Catalan Institute of Nanoscience and Nanotechnology (ICN2), CSIC, Barcelona Institute of Science and Technology, Campus UAB, Bellaterra, Barcelona, Spain

* nikolaos.mavredakis@uab.es

A. Supplementary Information: Thorough theoretical procedure for equations extraction

Generalized Noise Modeling methodology:

Under the assumption that the channel of the device is noiseless apart from an elementary slice between positions χ and $\chi+\Delta\chi$ as it is shown in Fig. 2b in the manuscript, the microscopic noise coming from this slice of the channel can be modeled as a local current source δI_n with a PSD $S_{\delta I^2 n}$ which is connected between χ and $\chi+\Delta\chi$ in parallel with the resistance of the slice ΔR (Norton equivalent) [43]. The transistor then can be split into two noiseless transistors M1 and M2 on each side of the local current noise source, at the source and drain side ends with channel lengths equal to χ and $L-\chi$ respectively. Since the voltage fluctuations on parallel resistance ΔR are small enough compared to thermal voltage U_T, small signal analysis can be used in order to extract a noise model according to which, M1 and M2 can be replaced by two simple conductances G_S on the source side and G_D on the drain side. The total channel conductance comes from the series connection of G_S and G_D as: $1/G_{CH}=1/Gs+1/G_D$[43]. The fluctuation of the current due to the local current noise source at the drain side δI_{nD} and its corresponding PSD $S_{\delta I^2 nD}$ are given by the following equations[43]:

$$\delta I_{nD} = G_{CH}\Delta R\delta I_n \qquad \text{(Eq. A1)}$$

$$S_{\delta I_{nD}^2}(\omega,x) = G_{CH}^2\Delta R^2 S_{\delta I_n^2}(\omega,x) \qquad \text{(Eq. A2)}$$

The PSD of the total noise current fluctuation at the drain side S_{ID} due to all different sections along the channel is obtained by summing their elementary contributions $S_{\delta I^2 nD}$ assuming that the contribution of each slice at different positions along the channel remains uncorrelated[43]:

$$S_{ID} = \int_0^L G_{CH}^2 \Delta R^2 \frac{S_{\delta I_n^2}(\omega, x)}{\Delta x} dx = \frac{1}{L^2} \int_0^L \Delta x S_{\delta I_n^2}(\omega, x) dx, \quad where\ G_{CH}^2 \Delta R^2 = \left(\frac{\Delta x}{L}\right)^2 \qquad \text{(Eq. A3)}$$

Carrier Number Fluctuation Effect:

As mentioned in the manuscript, the fluctuation of the trapped charge δQ_t can cause a variation in the chemical potential δV_c which can lead to a change to all charges that depend directly on chemical potential such as the graphene charge, the top gate and the back gate charge. The application of the charge conservation law gives:

$$\delta Q_{gr} + \delta Q_{top} + \delta Q_{back} + \delta Q_t = 0 \qquad \text{(Eq. A4)}$$

These induced fluctuations of the graphene, top gate and back gate charges can be related to the fluctuation of the chemical potential δV_c as[15, 43-46]:

$$\begin{aligned} \delta Q_{gr} &= -C_q \delta V_c \\ \delta Q_{top} &= -C_{top} \delta V_c \\ \delta Q_{back} &= -C_{back} \delta V_c \end{aligned} \qquad \text{(Eq. A5)}$$

If eqns (A4, A5) are taken into account then eqn (1) is transformed in eqn (3) in the manuscript. If the linear relationship between quantum capacitance and chemical potential mentioned in the manuscript, is integrated, charge of graphene can be calculated as:

$$Q_{gr} = \frac{k \cdot V_c^2}{2} + \rho_0 \cdot e \qquad \text{(Eq. A6)}$$

The PSD of the local noise source is calculated by eqn (4) in the manuscript. Taking the integral of this from Source to Drain in order to calculate the total 1/f noise PSD as in eqn (A3)[15, 43], we have:

$$\frac{S_{I_D}}{I_D^2} f \bigg|_{\Delta \mathrm{N}} = \frac{1}{L^2} \int_0^L \left(\frac{e}{Q_{gr}}\right)^2 \left(\frac{C_q}{C_{top} + C_{back} + C_q}\right)^2 \cdot \frac{KT\lambda N_T}{W} dx \qquad \text{(Eq. A7)}$$

In order to express this integral in terms of chemical potential V_c, we have to change the integral variable as[45-46]:

$$\frac{dx}{dV_c} = \frac{-\mu W Q_{gr}}{I_D} \frac{C_q + C_{top} + C_{back}}{C_{top} + C_{back}} \qquad \text{(Eq.A8)}$$

Where drain current is given as[45-46]:

$$I_D = \frac{\mu W k}{2L}\left[g\left(V_C\right)\right]_{Vcs}^{V_{cd}} \qquad \text{(Eq.A9)}$$

With $k=2\cdot e^3/(\pi\cdot h^2\cdot v^2 f)$[45-46] where vf is the Fermi velocity (=10^6 m/s) and h the reduced Planck constant (=$1,05\cdot 10^{-34}$ $J\cdot s$). Bias dependent term $g(V_c)$ is calculated as[45-46]:

$$\left[g\left(V_C\right)\right]_{Vcs}^{V_{cd}} = \frac{V_{cs}^3 - V_{cd}^3}{3} + \frac{k}{4\left(C_{top}+C_{back}\right)}\left[\mathrm{sgn}\left(V_{cd}\right)V_{cd}^4 - \mathrm{sgn}\left(V_{cs}\right)V_{cs}^4\right] + \frac{2\rho_0 e V_{DS}}{k} \qquad \text{(Eq.A10)}$$

eqn (A7) is transformed because of eqns (A8, A9, A10) to:

$$\left.\frac{S_{I_D}}{I_D^2} f\right|_{\Delta N} = \frac{4KT\lambda N_T e^2 k}{WL\left[g\left(V_c\right)\right]_{V_{cs}}^{V_{cd}}\left(C_{top}+C_{back}\right)}\int_{V_{cd}}^{V_{cs}} \frac{V_c^2}{\left(kV_c^2+2\rho_0 e\right)\left(C_{top}+C_{back}+k\left|V_c\right|\right)} dV_c \qquad \text{(Eq.A11)}$$

The integral in eqn (A11) can be solved analytically and gives the eqns (2, 5) in the manuscript.

Mobility Fluctuation Effect:

In the empirical Hooge model, the PSD of the local noise source is expressed as[43]:

$$\left.\frac{S_{\delta I_n^2}}{I_D^2}\right|_{\Delta\mu} = \frac{\alpha_H e}{Q_{gr} W \Delta x f} \qquad \text{(Eq.A12)}$$

If eqn (A12) is integrated along the channel as eqn (A3), the total noise PSD due to mobility fluctuations effect can be calculated as[43]:

$$\left.\frac{S_{I_D}}{I_D^2} f\right|_{\Delta\mu} = \frac{\alpha_H e}{WL^2}\int_0^L \frac{1}{Q_{gr}} dx \qquad \text{(Eq. A13)}$$

If eqn (A8) is applied in order to change the integration variable from x to V_c:

$$\left.\frac{S_{I_D}}{I_D^2} f\right|_{\Delta\mu} = \frac{\alpha_H e}{L^2 W\left(C_{top}+C_{back}\right)}\int_{V_{cd}}^{V_{cs}} \frac{\mu W Q_{gr}}{Q_{gr} I_D}\left(k\left|V_c\right| + C_{top} + C_{back}\right) dV_c \qquad \text{(Eq.A14)}$$

Where Q_{gr} is simplified in eqn (A14) and does not play a role in mobility fluctuation effect. If eqns (A9, A10) are also taken into account, then:

$$\left.\frac{S_{I_D}}{I_D^2} f\right|_{\Delta\mu} = \frac{2\alpha_H e}{WLk\left[g\left(V_c\right)\right]_{V_{cs}}^{V_{cd}}\left(C_{top}+C_{back}\right)}\int_{V_{cd}}^{V_{cs}} \left(k\left|V_c\right| + C_{top} + C_{back}\right) dV_c \qquad \text{(Eq.A15)}$$

The integral in eqn (A12) can be solved analytically and gives the eqns (6, 7) in the manuscript.

B. Supplementary Information Figure S1: Detailed examination of graphene charge along the channel.

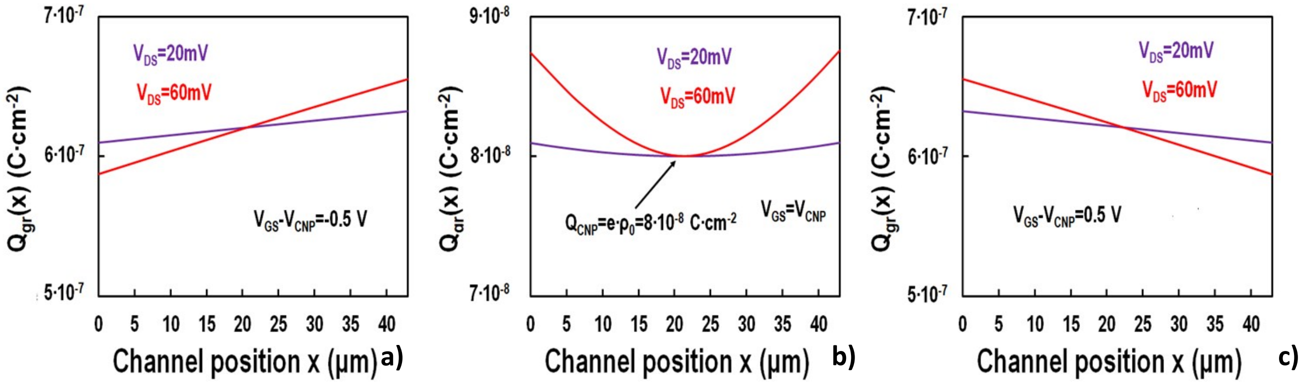

Figure S1. Graphene charge $Q_{gr}(x)$ vs. channel position x, for V_{GS}-V_{CNP} = -0,5 V (a), 0 V (CVP) b) and 0,5 V (c) at V_{DS} = 20, 60 mV for W/L=40 μm/43 μm.

Away from CNP (Fig. S1a-S1c), $Q_{gr}(x)$ is ~6-6.5·10^{-7} $C.cm^{-2}$ all along the channel for both drain voltage values. Considering the relative fluctuation of $Q_{gr}(x)$ from source terminal to the middle of the channel shown in Fig. 2c of the manuscript, the homogeneity of the channel is shown at high gate voltages for both V_{DS} values. Near CNP (Fig. S1b), $Q_{gr}(x)$ is equal to residual charge, $e\cdot\rho_0$, at $x=L/2$ for both high and low V_{DS}. This value remains almost constant throughout the channel for V_{DS}=20 mV but it is increased significantly for V_{DS}=60 mV confirming the inhomogeneous channel under these conditions.

C. Supplementary Information: Detailed examination of effect of residual charge in the M-shape bias dependence of 1/f noise.

If the procedure of the extraction of the theoretical equations regarding carrier number fluctuation effect takes place without considering residual charge, this can lead to very significant conclusions regarding the effect of residual charge on noise behavior. If residual charge is considered insignificant, then it must be eliminated in eqns (A6, A10). This results in the extraction of the following equation regarding 1/f noise due to carrier number fluctuation effect if the equivalent integral of eqn (A8) is solved:

$$\frac{S_{I_D}}{I_D^2} f\Big|_{\Delta N} = \frac{SD\big|_{\Delta N}\cdot KD\big|_{\Delta N}}{\left[g(V_c)\right]_{V_{cs}}^{V_{cd}}}, SD\Big|_{\Delta N} = \frac{2KT\lambda N_T e^2}{\left(C_{top}+C_{back}\right)kWL} \qquad \text{(Eq.A16)}$$

and $KD/_{\Delta N}$ is now given as:

$$\text{for } V_{cs,d}>0,\quad KD\Big|_{\Delta \mathrm{N}}=\Big[2\ln\big(C_{top}+C_{back}+kV_c\big)-4\ln\big(C_{top}+C_{back}\big)\Big]_{V_{cd}}^{V_{cs}}$$
$$\text{for } V_{cs,d}<0,\quad KD\Big|_{\Delta \mathrm{N}}=\Big[-2\ln\big(C_{top}+C_{back}-kV_c\big)\Big]_{V_{cd}}^{V_{cs}} \qquad \text{(Eq.A17)}$$

eqn (A17) is much simpler that eqn (2) of the manuscript. Regarding Hooge model, residual charge plays a role only in $g(V_c)$ factor in eqn (A10). As it can be seen in Fig. 3a of the manuscript, the omission of the residual charge lead to a Λ – shape behavior even for the carrier number fluctuation effect while the less the residual charge, the steeper Λ – shape trend with a higher maximum is observed for both carrier number and mobility fluctuation effects.

It would be very useful to observe how the absence of the residual charge affects both noise mechanisms ΔN and $\Delta\mu$ locally in the transistor channel. Regarding ΔN local noise model described by eqn (4) of the manuscript and $\Delta\mu$ local noise model described by eqn (A12), residual charge has an effect only in Q_{gr} as this is defined in eqn (A6). As it can be seen in Fig. S2, residual charge does not affect local noise at higher gate voltages for both noise mechanisms as it was expected (see Fig. 3a of the manuscript) since there ρ_0 does not affect significantly Q_{gr}. On the contrary at CNP, where ρ_0 approximately dominates Q_{gr}, the effect on local noise mechanisms is important. Fig. S2a shows the increase of ΔN local noise when ρ_0 is ignored leading to the Λ-shape of Fig. 3a of the manuscript. Similarly Fig. S2b shows the increase of $\Delta\mu$ local noise when ρ_0 is ignored.

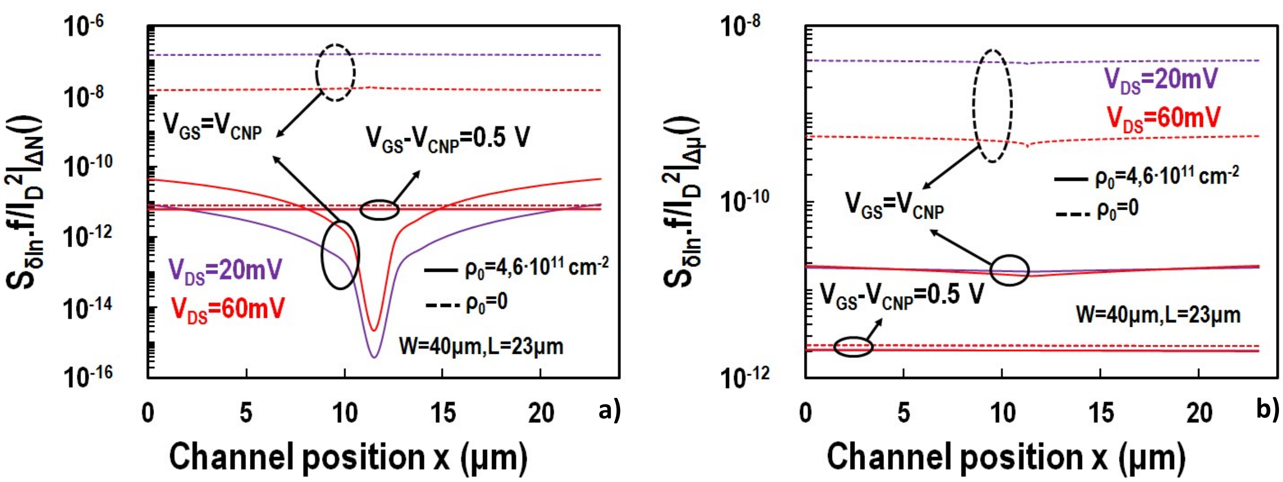

Figure S2. Normalized PSD of the local noise, $S_{\delta in}/I_D^2$, referred to $1\ Hz$, vs. channel potential x for ΔN (a) and $\Delta\mu$ (b) noise mechanisms.

D. Supplementary Information Figure S3: similar analysis with Fig. 4a and 4b of the manuscript but for the rest of the channel lengths

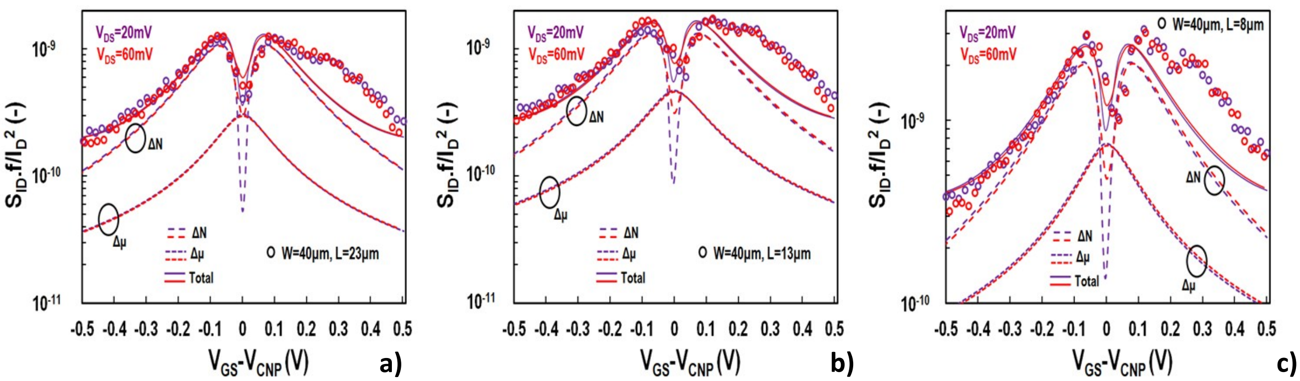

Figure S3. Output noise divided by squared drain current S_{ID}/I_D^2, referred to *1 Hz*, vs. top gate voltage overdrive $V_{GS} - V_{CNP}$, for liquid top-gated GFETs with $W=40\ \mu m$ for channel length $L=23\ \mu m$ (a), $L=13\ \mu m$ (b) and $L=8\ \mu m$ (c) at $V_{DS} = 20, 60\ mV$. markers: measured, solid lines: model, dashed lines: different noise contributions.

E. Supplementary Information: Derivation of an $(g_m/I_D)^2$ related LFN model with and without correlated mobility fluctuations

A very common approximation for modeling LFN in Si MOSFETs relates the output noise divided by squared drain current S_{ID}/I_D^2, with the squared transconductance to current ratio $(g_m/I_D)^2$ [15-16]. Despite the fact that this model is widely used in circuit simulators, is valid only under uniform channel conditions. This method has also been applied in Graphene FETs[4] and has been found to underestimate LFN at CNP where the channel is non-uniform even for a small V_{DS} as shown in Figure 2c of the main manuscript. In this section we will follow a similar approach as in References 15-17 in order to show how this model is extracted for Graphene FETs with and without the effect of correlated mobility fluctuations. For reasons of simplicity and since back gate voltage is not active in the devices used in this work, both back gate voltage and capacitance will be ignored.

Initially, we will show that the model proposed in Reference 16 ($S_{ID}/I_D^2= (g_m/I_D)^2.S_{Vfb}$) can be also applied in SLG FETs. From basic GFET electrostatics and if back gate is ignored we have:

$$Q_{gr}(x) = -C_t\left(V_{GS} - V_{GS0} + V_c(x)\right) \qquad \text{(Eq. A18)}$$

From Drift-Diffusion theory[43-45], we can assume that:

$$\Delta I_D = \frac{\mu W}{L}\int_{V_S}^{V_D} \Delta Q_{gr}(x) dV = \frac{\mu W}{L}\int_0^L \frac{dQ_{gr}(x)}{dV_{GS}} \frac{dV_{GS}}{dQ_t} \Delta Q_t \frac{dV}{dx} dx \qquad \text{(Eq. A19)}$$

From eqn (A18) we can conclude that $dV_{GS}/dQ_{gr}(x)=-1/C_t$ while if we assume that $KV_c>>qT$ which means that we are away from CNP and thus $C_q>>C_t$ then from eqns (1, 3) of the main manuscript we have $dQ_{gr}(x)/dQ_t=1$. So eqn (A19) becomes:

$$\Delta I_D = \frac{-\mu W}{L}\int_0^L \frac{dQ_{gr}(x)}{dV_{GS}} \frac{1}{C_t} \Delta Q_t \frac{dV}{dx} dx = \frac{-\mu W}{L}\int_0^L \frac{dQ_{gr}(x)}{dI_{DS}} \frac{dI_D}{dV_{GS}} \frac{1}{C_t} \Delta Q_t \frac{dV}{dx} dx \qquad \text{(Eq. A20)}$$

Again from Drift-Diffusion theory we have:

$$I_D = \mu W Q_{gr}(x) \frac{dV}{dx} \Rightarrow Q_{gr}(x) = \frac{-I_D}{\mu W \frac{dV}{dx}} \qquad \text{(Eq. A21)}$$

Under the assumption of a uniform channel where the graphene charge Q_{gr} and the electric field dV/dx are constant along it we have:

$$\frac{dQ_{gr}}{dI_D} = \frac{-1}{\mu W \frac{dV}{dx}} \qquad \text{(Eq. A22)}$$

From eqns (A20, A22) and since $d_{ID}/dV_{GS}=g_m$ we conclude:

$$\Delta I_D = \frac{1}{LC_t} g_m . e \int_0^L \Delta N_t dx \qquad \text{(Eq. A23)}$$

Which leads to:

$$\left.\frac{S_{I_D}}{I_D^2} f \right|_{\Delta \mathrm{N}} = \left(\frac{g_m}{I_D}\right)^2 \cdot \frac{q^2 KT \lambda N_T}{WLC_t^2} \qquad \text{(Eq. A24)}$$

The above eqn is exactly the same with eqn (9) of Reference 16 with the constant term to represent the flat band voltage fluctuations S_{VFb}. As we proved before, this model is valid only under uniform channel conditions and away from the CNP.

According to Reference 17, the model of eqn (A24) can be expanded including the correlated mobility fluctuations as:

$$\left.\frac{S_{I_D}}{I_D^2} f \right|_{\Delta \mathrm{N}} = \left(\frac{g_m}{I_D} + \alpha_c \mu C_t\right)^2 \cdot \frac{q^2 KT \lambda N_T}{WLC_t^2} \qquad \text{(Eq. A25)}$$

where α_c is the Coulomb scattering coefficient in *V.s/C* and μ is the mobility of the device. Figure S4 below presents the behavior of this simple approach described above with (eqn A25) and without (eqn A24) the effect of correlated mobility fluctuations for the shortest device with *L=5.5 μm* at V_{DS}*=20 mV* and V_{DS}*=60 mV*.

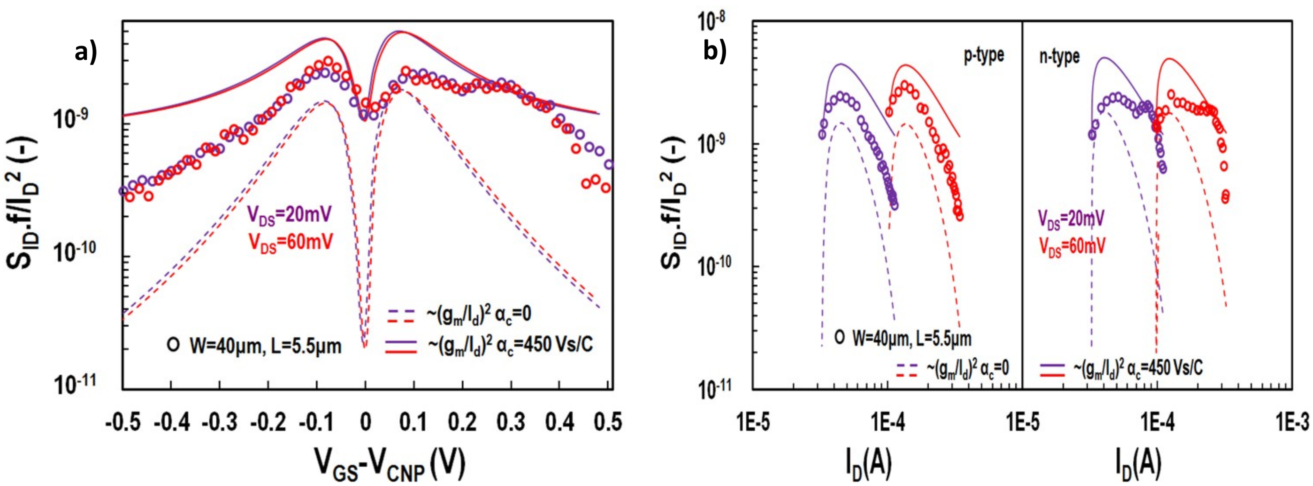

Figure S4. Output noise normalized with area and divided by squared drain current S_{ID}/I_D^2, referred to *1 Hz,* vs. top gate voltage overdrive $V_{GS} - V_{CNP}$ (a) and vs. drain current in both p- and n-type region (b) for liquid top-gated GFETs with *W/ L=40 μm / 5.5 μm* at V_{DS}*=20 mV* and V_{DS}*=60 mV*. markers: measured, solid lines: eqn (A25) model, dashed lines: eqn (A24) model.

Figure S4a presents the normalized S_{ID}/I_D^2 LFN vs top gate voltage overdrive $V_{GS} - V_{CNP}$ and what can be observed is that the model of eqn (A24) (α_c*=0*) underestimates LFN as it is also shown in Figure 4a of the manuscript for the longest device. Furthermore it is clear that the behavior of LFN is independent of V_{DS} even at the CNP because of the consideration of a uniform channel. If correlated mobility fluctuations model of eqn (A25) is activated then for a value of α_c*=450 Vs/C* the model captures the level of LFN at CNP still with no drain voltage dependence. But simultaneously the model overestimates LFN at higher gate voltages. Even if we assume that with an appropriate combination of α_c and α_H parameters we could achieve a better fitting, still the model would be independent of V_{DS} due to the homogeneous channel consideration.

Figure S4b presents the results of Figure 4a versus drain current I_D in log scale. Since I_D is symmetrical below (p-type) and above (n-type) CNP as it is shown in Figure 1c of the main manuscript, the two regions should be shown separately in log-scale. In an illustration similar to Figure S4b for Si MOSFETs, S_{ID}/I_D^2 LFN is maximum and constant in weak inversion region and decreases as we get deeper in strong inversion (See Figure 6 of Reference 17). Regarding weak inversion regime, this occurs because g_m/I_D

term is maximum and constant in the specific region and thus, eqn (A24) becomes equivalent to eqn (A25) since α_c is negligible. Consequently, N_T parameter which is included in S_{Vfb} term is extracted. As the drain current gets higher, LFN decreases and α_c parameter is extracted from this higher current regime. This is not the case in GFET though as it can be seen from Figure S4b since $(g_m/I_D)^2$ is not constant in lower current regime.

F. Supplementary Information Figure S5: normalized output noise with device area - WLS_{ID}/I_D^2

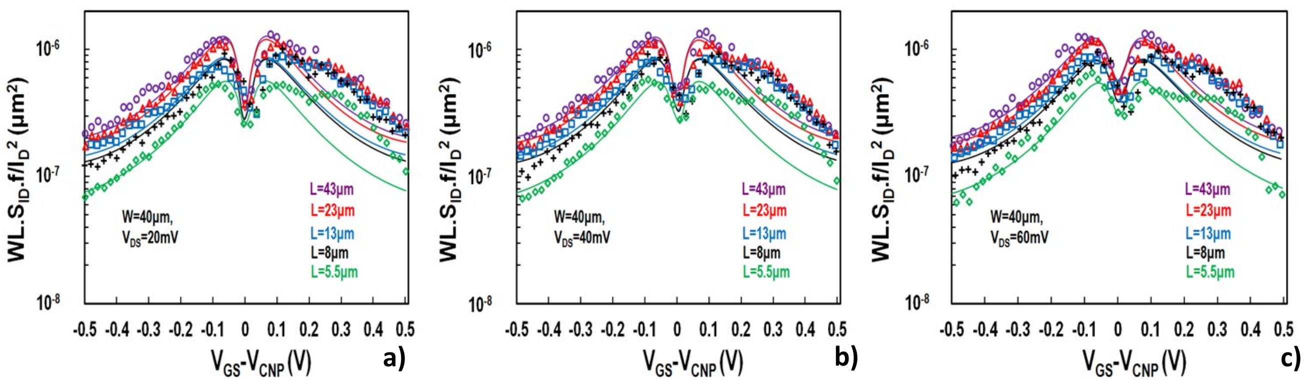

Figure S5. Output noise normalized with area and divided by squared drain current WLS_{ID}/I_D^2, referred to *1 Hz,* vs. top gate voltage overdrive $V_{GS} – V_{CNP}$ for liquid top-gated GFETs with $W=40\ \mu m$ for different channel length values ($L=43,\ 23,\ 13,\ 8,\ 5.5\ \mu m$) at $V_{DS}=20\ mV$ (a), $V_{DS}=40\ mV$ (b) and $V_{DS}=60\ mV$ (c). markers: measured, solid lines: model.